JOURNAL OF BIOMEDICAL OPTICS 1(3), 305–310 (JULY 1996)

DETECTION LIMIT IN LOCALIZING OBJECTS HIDDEN IN A TURBID MEDIUM USING AN OPTICALLY SCANNED PHASED ARRAY

D. G. Papaioannou, G. W. 't Hooft, S. B. Colak, and J. T. Oostveen
Philips Research Laboratories, Prof. Holstlaan 4, 5656 AA Eindhoven, The Netherlands
(Paper JBO-055 received Nov. 14, 1995; revised manuscript received Mar. 25, 1996; accepted for publication Apr. 30, 1996)

ABSTRACT

In this paper the sensitivity of a phased array and a continuous wave measurement setup are compared. Both techniques are used to image inhomogeneities hidden inside a tissuelike turbid medium. We have found that despite the higher technical complexity of the phased array measurement, its sensitivity in detecting inhomogeneities is virtually the same as the sensitivity of the continuous wave measurement. *© 1996 Society of Photo-Optical Instrumentation Engineers.*

Keywords phased array; medical imaging; turbid media; detection limit.

1 INTRODUCTION

In localizing inhomogeneities embedded within a highly scattering medium, various optical methods are available. The simplest approach is to use a point source of continuous light and measure the light distribution at the circumference of the turbid medium.[1–3] By varying the input source position, one obtains tomographic data and by backprojection image results of the attenuation coefficient, k_{DC}, given by

$$k_{DC}=\sqrt{3\mu_a\mu_s'}\ , \tag{1}$$

where μ_a is the absorption coefficient and μ_s' is the reduced, or transport-corrected scattering coefficient of the light. Owing to the diffuse nature of the light, the picture is blurred, i.e., a point inhomogeneity appears smeared out primarily along the transverse direction of the transillumination axis. By iterative techniques or deconvolution methods, the resolution can be improved considerably.[3–5]

A second method makes use of so-called photon density waves,[6–9] i.e., the light source is amplitude modulated (AM) and the detector(s) picks up the intensity of the modulated light and its phase. In this way, an image may result for the attenuation coefficient, k_{AC}, which equals:

$$k_{AC}=\sqrt{\frac{\mu_a\nu-i\omega}{D}}, \tag{2}$$

where ν is the velocity of the light in the medium, ω the angular frequency, and D the diffusion coefficient of the light, i.e., $D=1/[3(\mu_a+\mu_s')]$. This method has two advantages with respect to continuous wave techniques. First, by evaluating the real and imaginary part of the attenuation coefficient, both the absorptive effects and scattering effects can be disentangled, thereby characterizing the medium in a better way. Second, for sufficiently large modulation frequencies, the AC attenuation coefficient, k_{AC}, can be increased substantially with respect to its DC counterpart. Hence, the intrinsic image resolution is improved. Whether the actual AC resolution is still superior after deblurring with convolution techniques remains to be seen, however. The price to be paid is that these two improvements are more complicated, and therefore have less cost-effective electronics. Furthermore, due to the higher attenuation coefficient, the signal levels on the detectors will be exponentially smaller. Note that the signal strength scales with the diffusive photon density, Φ, which equals at a source detector distance r in an infinite medium:

$$\Phi=\frac{S_0}{4\pi Dr}\exp(-kr), \tag{3}$$

where S_0 is the source strength and k the appropriate attenuation coefficient.

This paper compares the ability to detect small objects embedded in a turbid medium intrinsic to the various optical methods. In this respect, an intriguing extension of the photon density approach has been proposed by Chance et al.[10,11] using a phased array of sources. In this method, two spatially separated point sources with the same modulation frequency are employed. By making the second source antiphase with respect to the first one, a symmetry plane is created that bisects the source-

E-mail: thooft@natlab.research.philips.com

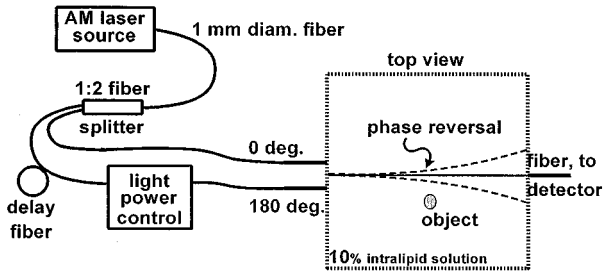

Fig. 1 Schematic of the phased array setup in which optical scanning of the phase reversal position is incorporated. The solid line in the scattering media directed toward the detection fiber denotes the symmetry plane in the absence of inhomogeneities and for equal powers of the in-phase and antiphase source. At this plane the phase of the modulation changes by 180 deg and the modulation depth is minimal. The dashed lines represent the influence of an inhomogeneity on the symmetry line and how this can be counterbalanced by adjusting the power ratio of the two sources.

source line. At this symmetry plane, the modulation depth of the diffusive light is negligible and the phase of the modulation changes from 0 to 180 deg. We will call this the *phase reversal region*. In Figure 1 a schematic of the technique is depicted. The solid line represents the symmetry plane. When an inhomogeneity is present, the symmetry is broken and the plane at which the phase of the modulation changes is bent (the dashed, curved lines in Figure 1). A detector at the original symmetry plane will measure an increased modulation depth and a shifted crossover from 0 to 180 deg of the phase. By changing the power ratio of the two sources, the detector readings can be restored, i.e., a minimum in modulation depth and a phase reversal at the detector. By scanning the assembly of two sources and a detector along the turbid medium and constantly adjusting the power ratio of the sources, the exact position of an object can be determined. This method of locating an object is a null experiment. Variations in the power ratio will only occur with the presence of inhomogeneities. Therefore, the ability to detect an object with this technique is expected to be great. The purpose of this paper is to establish this sensitivity and compare it with that resulting from continuous wave transmission measurements.

2 EXPERIMENTAL SETUP

Figure 1 depicts the schematic outline of the experimental setup using a phased array. A passive amplitude-modulated Ti:sapphire laser is used as the light source for the phased array configuration. Passive amplitude modulation of a laser can be achieved by placing an etalon into the laser cavity, allowing only two adjacent modes to exist. The two modes beat with one another, producing an amplitude modulation of the laser light intensity, I:

$$I=|E_1\exp(i\omega t)+E_2\exp[i(\omega+\delta\omega)t]|^2$$
$$=E_1^2+E_2^2+2E_1E_2\cos(\delta\omega t). \quad (4)$$

The frequency of the amplitude modulation is equal to the mode separation, which for our laser is 219 MHz. The advantages of using a passive amplitude-modulated laser are the following: First, no radio-frequency (RF) interference is present since no RF source is used, as in the case of direct AM of a laser diode; the absence of RF interference removes a significant burden from the detection electronics which handle in general very small signals. Second, the modulation produced is very clean with a suppression of harmonics better than 65 dB; this suppression is not possible with direct modulation of a laser diode. Third, the depth of the modulation is close to one, and is determined by measuring the amplitudes $|E_1|^2$ and $|E_2|^2$ of the two modes with a scanning Fabry-Perot spectrum analyzer. Their magnitudes are equal to within 5% ($|E_1|^2/|E_2|^2=0.95$; consequently the modulation depth of the laser AC/DC=$2E_1E_2/(|E_1|^2+|E_2|^2)$ ≈ 1.0.

Light from the laser is coupled into a multimode (1 mm diameter), 50–50% fibersplitter (see Fig. 1). In the one branch of the fibersplitter, an extra piece of fiber is added to create a 180 deg phase difference in the modulation of the light of the two branches. By using this ''delay'' fiber, we can very accurately set the phase difference between the two branches. Light from one of the fibers is passed through a polymer-dispersed, liquid-crystal light valve that controls the light intensity ratio between the two fiber outputs. The two fiber outputs, separated by 10 mm, are placed in a fishtank filled with a 10 solution of stock intralipid (corresponding to the commercial product Intralipid-10% diluted 10 times). The reduced scattering and absorption coefficients of our intralipid solution are $\mu_s'=1.2\ \text{mm}^{-1}$ and $\mu_a<0.005\ \text{mm}^{-1}$, respectively.[12]

The detector fiber is placed at a distance of 50 mm from the source fibers. A photomultiplier tube (PMT) with a total bandwidth of 300 MHz is used to detect the light transmitted through the turbid medium. The output of the PMT is amplified, downconverted to a few hundreds of Hertz, and fed to a phase/gain meter which determines the AC component and the phase. The schematics of the electronics to perform these measurements are shown in Figure 2. The downconversion of the detector signal (measured) to a lower frequency is done in a mixer using an extra local oscillator signal that is frequency shifted and phase locked. This signal is obtained from a reference photodiode signal monitoring the laser modulation. With the aid of two mixers and two phase-locked signal generators, this reference signal at 219 MHz is converted to a reference signal of 219 MHz+400 Hz. This new reference signal still follows the frequency drift of the modulation of the laser and is used to mix both

the PMT signal and the original reference signal down to 400 Hz. These two low-frequency signals are filtered and fed to the phase/gain meter. The noise level of this total system corresponds to an optical input signal at the detector fiber of only 0.7 pW. The accuracy of the phase measurement is 0.2 deg for AC signals that are 13 dB or more above the noise level. At sufficient power levels, the relative accuracy of the AC amplitude is approximately $5\text{x}10^{-3}$. In the nulling method described above, the accuracy of the power ratio of the two out-of-phase input sources determines the sensitivity of the system to the presence of inhomogeneities. This accuracy amounts to about 0.3%.

For DC measurements, the two input fibers are replaced by a single fiber, which is fed with the light from a continuous-wave semiconductor laser. The electronics of the photomultiplier are replaced by an electrometer. The noise equivalent power of this system is approximately 50 fW of optical power at the detection fiber. The sensitivity to the presence of inhomogeneities, however, is determined by the variance of the detector current. This accuracy amounts to approximately 0.2%.

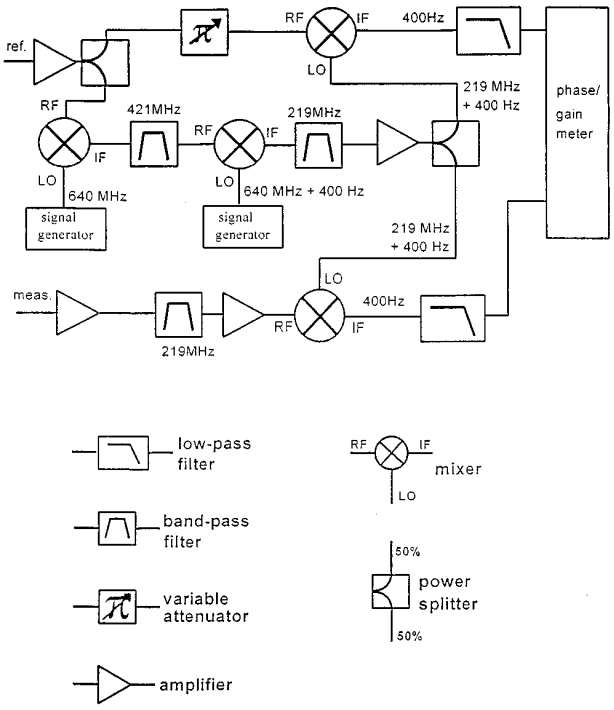

Fig. 2 Schematic drawing of the downconversion electronics. In order to measure the amplitude and phase of low light levels at 219 MHz, the signals are downconverted in frequency using RF mixers. The 400-Hz shifted reference signal is derived from a 219-MHz signal coming from a photodiode monitoring the laser modulation.

3 EXPERIMENTAL RESULTS AND DISCUSSION

With the phased array setup we have achieved detection and localization of metal wires as small as 0.5 mm in diameter, hidden in the middle of a 50-mm thick–10% intralipid solution. For biomedical applications, however, detection of wires, even as small as 0.5 mm, is of no interest. Consequently, we have selected white Delrin (Delrin®≡ polyoxymethylene) as a material to make objects that mildly disturb the homogeneity of the intralipid solution. The reduced scattering and absorption coefficients for white Delrin are μ_s'=2.2 mm^{-1}, μ_a<0.005 mm^{-1}, respectively, with the first being about twice the corresponding value for the intralipid solution. The white Delrin objects are 80-mm long cylinders of various diameters, aligned perpendicular to the plane containing the two sources and the detector, and located midway between the source and detector. The source–detector separation is 50 mm. The source and detector are scanned through the fishtank simultaneously. In Figure 3 we plot the phase of the detected light, represented by different colors (see color code of Figure 3), as a function of the position of the combined phased array and detector (y axis), and the power ratio of the two sources (x axis). A 10-mm-diameter white Delrin cylinder is present in the turbid medium. The black solid line denotes the power ratio to align the phase-reversal position at the detection fiber. The ''wiggle'' of the power ratio as a function of the position reveals the presence of the Delrin cylinder.

At the plane of the phase reversal, the AC component is ideally zero (practically equal to the noise level of the detection configuration for a perfectly balanced phased array). As mentioned in the introduction, an alternative way to detect the presence of an inhomogeneity is to measure the power ratio of the two sources that causes the detector to read a minimum AC component. The values of the AC component as a function of the position of the combined phased array and detector (y axis), and the power ratio of the two sources (x axis) are presented in Figure 4. The black solid line indicates the position of the minimum AC value. The advantage of the phase-reversal measurement is that it represents a steep transition from a phase value ϕ to a phase value 180 deg+ϕ. The disadvantages are the following: First, the accuracy of the phase measurement close to the phase-reversal regime is quite low because the AC component is rather small, and second the phase-gain meter can only measure phases in the range 0 to +360 deg; consequently, phase values 360 deg+ϕ are wrapped down to ϕ, which makes the manipulation of the data complex. On the other hand, the advantage of the AC-minimum is that the AC value can be measured quite accurately; the disadvantage of this approach is that the AC-minimum region is quite broad. By observing the data in Figures 3 and 4, we can see that use of

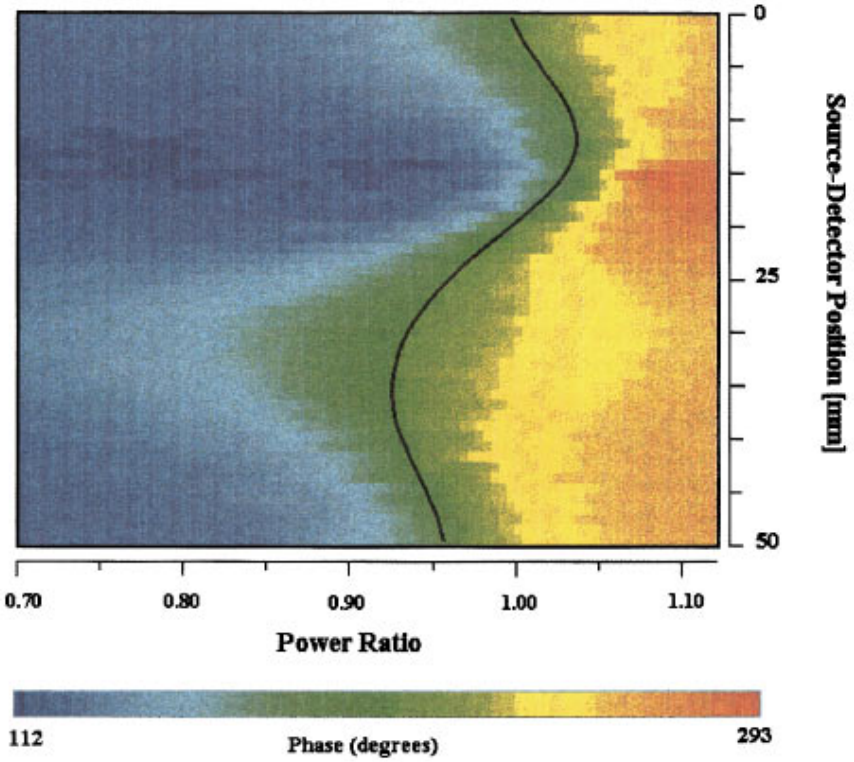

Fig. 3 Phase of the amplitude modulation of the detected light, represented by different colors, as a function of the position of the combination of the phased array and detector (*y* axis), and the power ratio between the two sources (*x* axis). The color code is in a linear scale ranging from 112 to 293 deg.

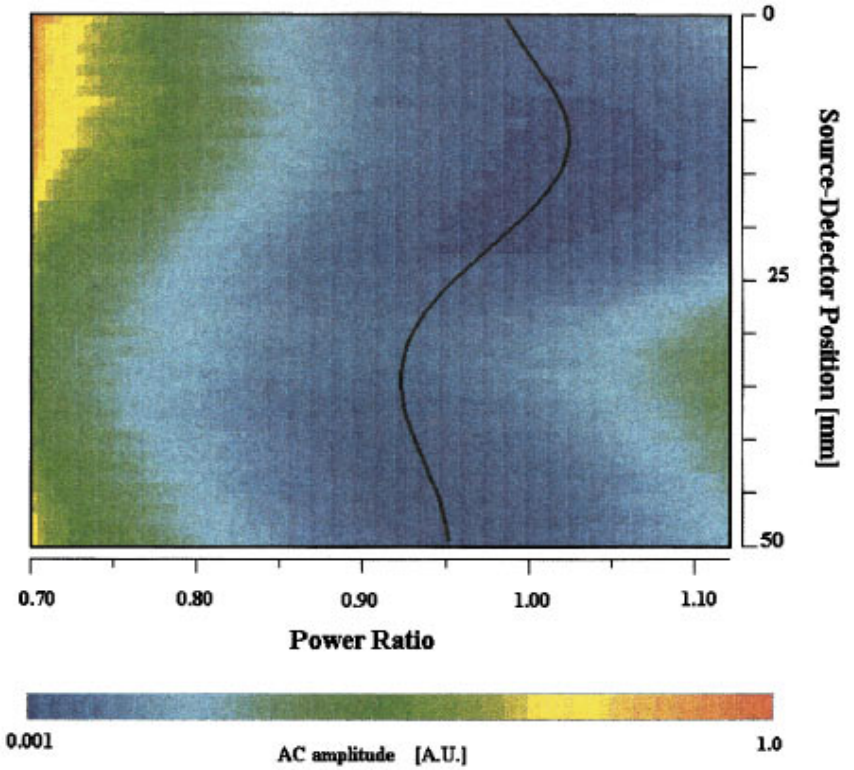

Fig. 4 AC component of the detected light, represented by different colors, as a function of the position of the combined phased array and detector (*y* axis), and the power ratio between the two sources (*x* axis). The color-code is in a linear scale ranging from 0.001 to 1.

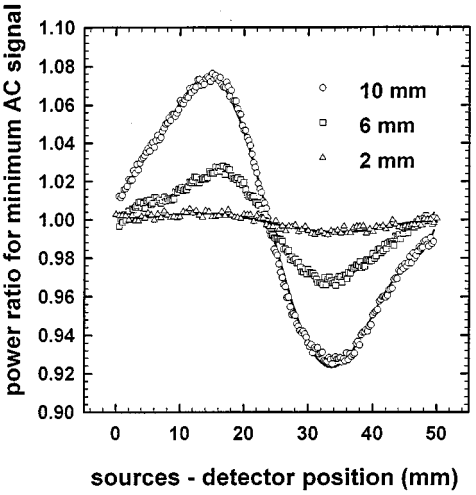

Fig. 5 Power ratio at which AC minimum occurs, as a function of the source-detector position. The source-detector separation is 50 mm; the turbid medium is a 10% intralipid solution; and the objects are 80-mm-long white Delrin cylinders of various diameters.

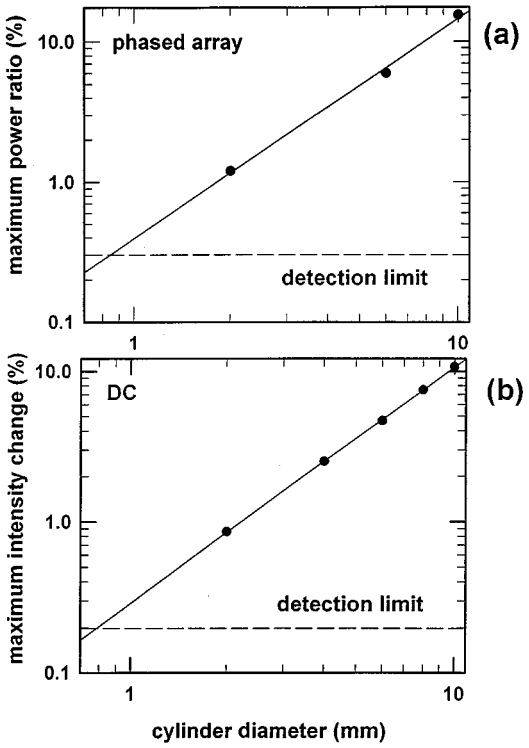

Fig. 6 (a) Double logarithmic plot of maximum power ratio adjustment derived from the data of Fig. 5, as a function of the Delrin cylinder diameter. The horizontal line denoted ''detection limit'' corresponds to the accuracy level of the power ratio. (b) Double logarithmic plot of the light intensity difference between the presence and absence of a white Delrin cylinder as a function of the cylinder diameter. The horizontal line denoted ''detection limit'' corresponds to the accuracy level of the DC measurement. The source-detector separation is 50 mm; the turbid medium is a 10% intralipid solution; and the objects are 80-mm-long white Delrin cylinders of various diameters.

either the phase reversal or the AC minimum yields practically the same accuracy of the adjusted power ratio of 0.3%. The sensitivities to the presence of an inhomogeneity are the same. A preferred choice is the AC-minimum approach which is more straightforward from a data manipulation point of view. In Figure 5 we plot the power ratio for which the detector reads a minimum AC signal as a function of the position of the combined phased array and detector for three Delrin cylinder diameters (10, 6, and 2 mm). The power ratio had to be adjusted in a sinusoidal-like way while scanning. When the object traverses the straight line from the first source to the detector, the power ratio is at a maximum, while the minimum is reached at the line from the second source to the detector. The separation of the positions of the maximum and minimum is determined by the geometry of the setup, i.e., the separation of the sources and their distance to the detector. The values of the extremes are a measure of the magnitude of the disturbance, i.e., the physical size of the object as well as its difference in attenuation coefficient compared with the surrounding medium.

In Figure 6(a) we present the maximum power ratio adjustment as a function of the object diameter in a double logarithmic plot. Our setup with 80-mm-long samples vertically placed midway between sources and detector resembles a two-dimensional geometry. We therefore would expect a variation of the measured effect that is proportional to the square of the object's diameter. From Figure 6(a) we infer a slope of 1.6. For small scattering objects, the slope should decrease owing to a refractive index step which changes the boundary conditions for the photon density waves.[13] We are not able (yet) to quantitatively calculate the effect for our geometry. The extrapolated line through the data of Figure 6(a) crosses the detection limit of 0.3% at an object diameter of about 0.8 mm. For our equipment with a source detector distance of 50 mm, this is the smallest 2-D object that can be observed.

With the same sample parameters (10% intralipid solution, Delrin cylinders of various diameters, 50 mm source–detector separation) we perform measurements using a continuous wave (CW) light source instead of a phased array. The Delrin cylinder is placed midway between source fiber and detector fiber. The detected light intensity, compared with the light intensity in the absence of the disturbance, is simply a measure of the sensitivity of the imaging approach. The results for various Delrin cylinder diameters are plotted in Figure 6(b). In this double logarithmic plot, again a straight line is obtained with slope 1.6 which is in perfect agreement with the phased array measurements. Since the accuracy in the DC light intensity is similar, the minimum object size is also approximately 0.8 mm. Moreover, at a given object diameter, the relative change in the measured DC signal of Figure 6(b)

almost equals the relative adjustment of the power ratio of the phased array measurements of Figure 6(a). At first glance, this is somewhat surprising since the relative variation of the intensity owing to the presence of a *scattering* object should scale with $(1+kr)^2$. This gives rise to a 1.7 times larger relative effect at 219 MHz than at DC. (Note that for *absorbers* there is no influence of the modulation frequency on the relative variation of the intensity.) The advantage of the larger attenuation coefficient is partially compensated for by the fact that in the phased array technique, the maximum power ratio adjustment is obtained when the object is asymmetrically aligned, thereby decreasing the influence of at least one source-detector combination.

4 SUMMARY

We have investigated the sensitivity of an optically scanned phased array and CW technique, to image the interior of a turbid medium. The optical parameters of the turbid medium were chosen to be similar to the ones of breast tissue. Low-contrast inhomogeneities (only a factor of 2 larger reduced scattering coefficient) made out of white Delrin were embedded inside the turbid medium; inhomogeneities of various sizes were imaged using both techniques. We found that both techniques have about the same sensitivity in detecting and localizing the inhomogeneities. In the steady progress of science and technology, one might expect that in the future the performance of optical detectors and electronics will improve. With an increased accuracy, the ability to detect small inhomogeneities will also be enhanced. It would, however, be very surprising if the improvement in RF electronics were to be substantially superior than that in ''simple'' DC measurements. The conclusion that both types of techniques appear to be comparable in their ability to detect objects is likely to hold also in the near future.

The modulation depth at the detector decreases exponentially with source-detector distance, viz. $\exp[(k_{DC} - k_{AC})r]$. Consequently, for very large distances, the noise from the detector due to the relatively large DC signal at the modulation frequency of the photon density waves will influence the accuracy of the AC signal and its phase measurement. The larger the modulation frequency, the smaller the distance when this occurs. For our setup, the modulation depth at a source-detector distance of 70 mm using 219 MHz is still sufficient proper measurements.

We would like to note, however, that the AM light sources used in the phased array have the advantage that they can offer extra information (such as the absolute value of the AC component and the phase), which can be used to determine both the absorption and the scattering coefficient as a function of position in the sample; in contrast, the CW measurement can yield information only on the extinction coefficient k_{DC}, i.e., the combined effect of the absorption and scattering coefficients.

Acknowledgments

The authors would like to acknowledge the valuable contributions of M. Koelink, M. B. van der Mark, and J. Paasschens for numerous stimulating discussions on the material of this paper.

REFERENCES

1. Y. Yamashita and M. Kaneko, ''Visible and infrared diaphanoscopy for medical diagnosis,'' in *Medical Optical Tomography: Functional Imaging and Monitoring*, G. Müller et al., Eds. Vol. **IS11**, pp. 283–316 (1993).
2. S. Zhao, M. A. O'Leary, S. Nioka, and B. Chance, ''Breast tumour detection using continuous light source,'' *Proc. SPIE* **2389**, 809–817 (1995).
3. S. B. Colak, G. W. 't Hooft, D. G. Papaioannou, and M. B. v.d. Mark, ''Optical image reconstruction with deconvolution in light diffusion media,'' *Proc. SPIE* **2626** (1996).
4. J. Chang, H. L. Grabor and R. L. Barbour, ''Image reconstruction of targets in random media from continuous wave laser measurements and simulated data,'' in *OSA Proceedings on Advances in Optical Imaging and Photon Migration*, R. R. Alfano, Ed., OSA **21**, pp. 193–201 (1994).
5. S. C. Feng, H.-L. Zhao, and F.-A. Zeng, ''A new algorithm for near infrared diffuse photon imaging in human tissue,'' *Proc. SPIE* **2389** 113–119 (1995).
6. M. A. O'Leary, D. A. Boas, B. Chance, and A. G. Yodh, ''Refraction on diffuse photon density waves,'' *Phys. Rev. Lett.* **69** 2658–2661 (1992).
7. J. B. Fishkin and E. Gratton, ''Propagation of photon-density waves in strongly scattering media containing an absorbing semi-infinite plane bounded by a straight edge,'' *J. Opt. Soc. Am.* **A10** 127–140 (1993).
8. B. J. Tromberg, L. O. Svaasand, T.-T. Tsay, and R. C. Haskell, ''Properties of photon density waves in multiple-scattering media,'' *Appl. Opt.* **32** 607–616 (1993).
9. S. Fantini, M. A. Franceschini, G. Gaida, E. Gratton, H. Jess, W. W. Mantulin, U. T. Moesta, P. M. Schlag, and M. Kaschke, ''Frequency domain optical mammography: edge effect corrections,'' *Med. Phys.* **23** 149–157 (1996).
10. B. Chance, K. Kang, L. He, J. Weng, and E. Sevick, ''Highly sensitive object location in tissue models with linear in-phase and anti-phase multi-element optical arrays in one and two dimensions,'' *Proc. Natl. Acad. Sci. U.S.A.* **90** 3423–3427 (1993).
11. B. Chance, ''Multi-element phased arrays for phase modulation imaging,'' *Proc. SPIE* **1888** 354–358 (1993).
12. D. G. Papaioannou, G. W. 't Hooft, J. J. M. Baselmans, and M. J. C. van Gemert, ''Image quality in time-resolved transillumination of highly scattering media,'' *Appl. Opt.* **34** 6144–6157 (1995).
13. J. C. J. Paasschens, private communications.